

SUPPLEMENTAL MATERIALS AND METHODS

Analysis of GST-core RAG2 by MALLS

MALLS SEC was performed as previously described (1,2). Briefly, GST-core RAG2 protein was loaded onto a 200 HR 10/30 gel filtration column (Amersham Pharmacia, Piscataway, NJ). The column buffer was comprised of 20 mM Tris pH 8.0, 5 mM β -mercaptoethanol (BME), and 0.2 M NaCl. Analysis of eluant was performed using a DAWN DSP laserphotometer coupled with an Optilab DSP interferometric refractometer (Wyatt Technology, Santa Barbara, CA). Astra 4.72 software was used to perform the molecular mass calculations. The value for dn/dc was set at 0.19 for the molecular mass calculations, as previously described (1). Aliquots from selected fractions were analyzed by Western blotting to detect GST-core RAG2 as previously described (3).

Complete tryptic digestion of MBP-core RAG1 and GST-core RAG2

MBP-core RAG1 and GST-core RAG2 were expressed and purified as described in the text. MBP-core RAG1 (1 μ g) was incubated with 7 mM iodoacetamide for 15 min at ambient temperature in 20 mM Tris-HCl pH 8.0, 50 mM NaCl, 10 μ M ZnCl₂, and 20 mM β -mercaptoethanol. GST-core RAG2 (1 μ g) in 25 mM Tris-HCl, pH 8.0, 150 mM KCl, and 2 mM dithiothreitol was incubated with iodoacetamide as above. Subsequently, the modified proteins were incubated with 0.04 μ g porcine pancreatic trypsin (Sigma) at 37°C for 20 hours. The digested products were desalted and purified by a C18 ZipTip (Millipore) and the peptides subsequently eluted in 50% acetonitrile and 0.1% TFA. MBP-core RAG1 and GST-core RAG2 peptide samples were separately spotted on a grid with an equal volume of α -cyano-4-hydroxycinnamic acid, and analyzed by the Voyager Elite MALDI-TOF mass spectrometer (Applied Biosystems, Framingham, MA) at the National Science Foundation Experimental Program to Stimulate Competitive Research (NSF-Epscor) Oklahoma Laser Mass Spectrometry facility.

Fluorescence Microscopy

HeLa cells were seeded onto glass coverslips in 6 well plates and grown to 80% confluency prior to transfection. Next, plasmids encoding GFP-core RAG1 (WT or mutant) were transfected (4 μ g of plasmid per well) using Lipofectamine 2000 (Invitrogen; Carlsbad, CA). Following 24 hrs, cells were washed with PBS and fixed in 2% PFA for 20 min at room temperature. Cells were subsequently washed with PBS containing 10 mM glycine (PBS-glycine), then stained with 300 nM 4',6-diamidino-2-phenylindole (DAPI) in PBS-glycine. Fluorescence imaging was performed using a Nikon Eclipse E400 epifluorescence microscope equipped with a DP70 camera, and filter sets for detection of DAPI and GFP fluorescence. Excitation (ex) and emission (em) wavelengths for imaging were 325-375 nm (ex) and 435-485 nm (em) for DAPI, and 465-495 nm (ex) and 515-555 nm (em) for GFP. Image processing was performed using iVision (BioVision Technologies, Exton, PA).

GFP-trap assay

GFP-trap assays were performed as described in the main text for the RFP-trap assay with the following exception. Aliquots of lysates containing equivalent amounts of GFP-core RAG1 (based on readout from the fluorescence microplate reader) were incubated overnight at 4°C with 10 μ l magnetic beads that were linked by camelidae antibody specific to green fluorescence protein, referred to as GFP-trap magnetic beads (Chromotek). Remaining steps were as described in the main text.

Quantification of Ch-FL-RAG2 and GFP-core RAG1 in cell lysates used for fluorescence-based pull down assay

293T cell lysates containing co-expressed Ch-FL-RAG2 and GFP-core RAG1 were placed in 96 well plates, and the relative amount of each fluorescently tagged protein determined using a fluorescence microplate reader (POLARstar Omega plate reader, BMG Labtech). The samples used in the RFP-trap and GFP-trap pull down assays were normalized relative to the amount of Ch-FL-RAG2 and GFP-core RAG1, respectively. For each sample, lysate containing Ch-FL-RAG2 corresponding to 50,000

counts was added for loading the RFP-trap beads; and lysate containing GFP-core RAG1 corresponding to 50,000 counts was added for loading the GFP-trap beads.

REFERENCES

1. Godderz LJ, Peak MM, Rodgers KK (2005) Analysis of biological macromolecular assemblies using static light scattering methods. *Curr Org Chem* 9:899-908.
2. Godderz LJ, Rahman NS, Risinger GM, Arbuckle JL, Rodgers KK (2003) Self-association and conformational properties of RAG1: Implications for formation of the V(D)J recombinase. *Nucleic Acids Res* 31:2014-2023.
3. Arbuckle JL, Fauss LJ, Simpson R, Ptaszek LM, Rodgers KK (2001) Identification of two topologically independent domains in RAG1 and their role in macromolecular interactions relevant to V(D)J recombination. *J Biol Chem* 276:37093-37101.
4. De P, Zhao S, Gwyn LM, Godderz LJ, Peak MM, Rodgers KK (2008) Thermal dependency of RAG1 self-association properties. *BMC Biochem* 9:5. PMID: 18234093 {Medline}

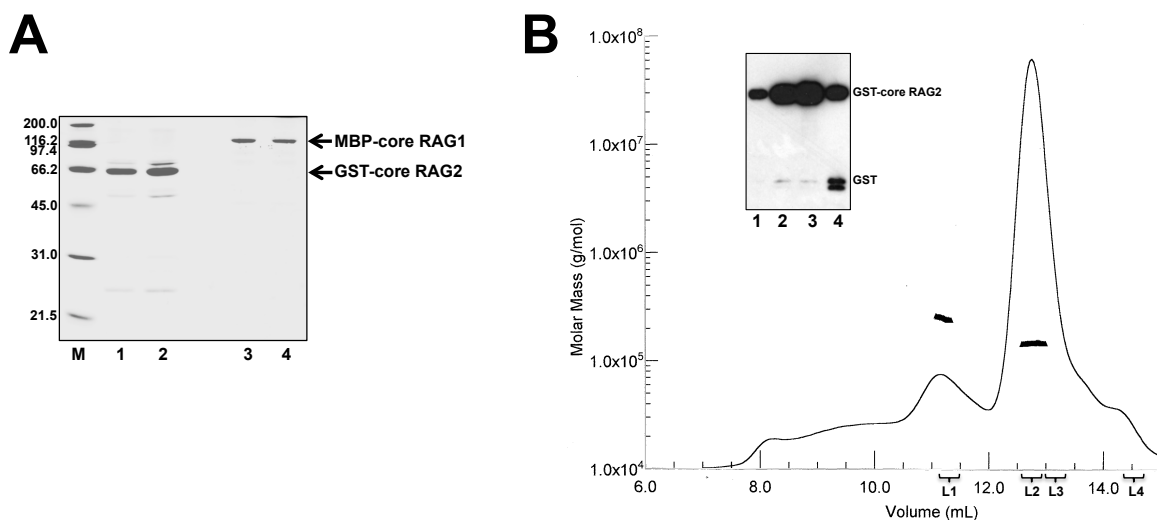


Figure S1: Analysis of purified core RAG proteins **(A)** Silver stained 12% polyacrylamide SDS gel of purified GST-core RAG2 and MBP-core RAG1. Molecular weight markers are in lane 1, with masses (in kD) of each marker at the left of the gel. Note that the 116.2 kD and 97.4 kD standards migrate as a close doublet in the gel. Purified GST-core RAG2 (expressed and purified from 293T cells at concentrations of 3.0 and 4.0 μ M are in lanes 2 and 3, respectively. MBP-core RAG1 (purified from *E. coli*) at concentrations of 0.9 and 0.7 μ M are in lanes 4 and 5, respectively. **(B)** Analytical gel filtration chromatography profile of GST-core RAG2 analyzed by multi-angle laser light scattering, using methods previously described (1). The profile of a purified sample of GST-core RAG2 from a Superdex 200 gel filtration column as monitored by a refractometer detector. The thick black lines above peaks A and B are the molecular masses measured by multi-angle laser light scattering (MALLS) as the protein eluted from the column. Peak A consisted of protein with molecular masses in the range of 200-300 kD, and likely represents a mixture of dimeric and tetrameric GST-core RAG2. The majority of protein eluted in peak B as a monodisperse species with a mass of 146 ± 10 kD, consistent with dimeric GST-core RAG2 (at an expected mass of 138 kD). Inset gel: α -GST Western blot of fractions collected from the column. Lanes 1-4 in the blot corresponds to material collected in L1-L4, respectively, denoted below the elution profile. Lane 1 is from protein in Peak A, and lanes 2-3 is dimeric GST-core RAG2 protein eluting in Peak B. Lane 4 is material eluting in a minor shoulder of Peak B, which contains GST-core RAG2, and GST, with the GST resulting from minor degradation of the fusion protein. MALLS-SEC of MBP-core RAG1 has been previously described (1,4).

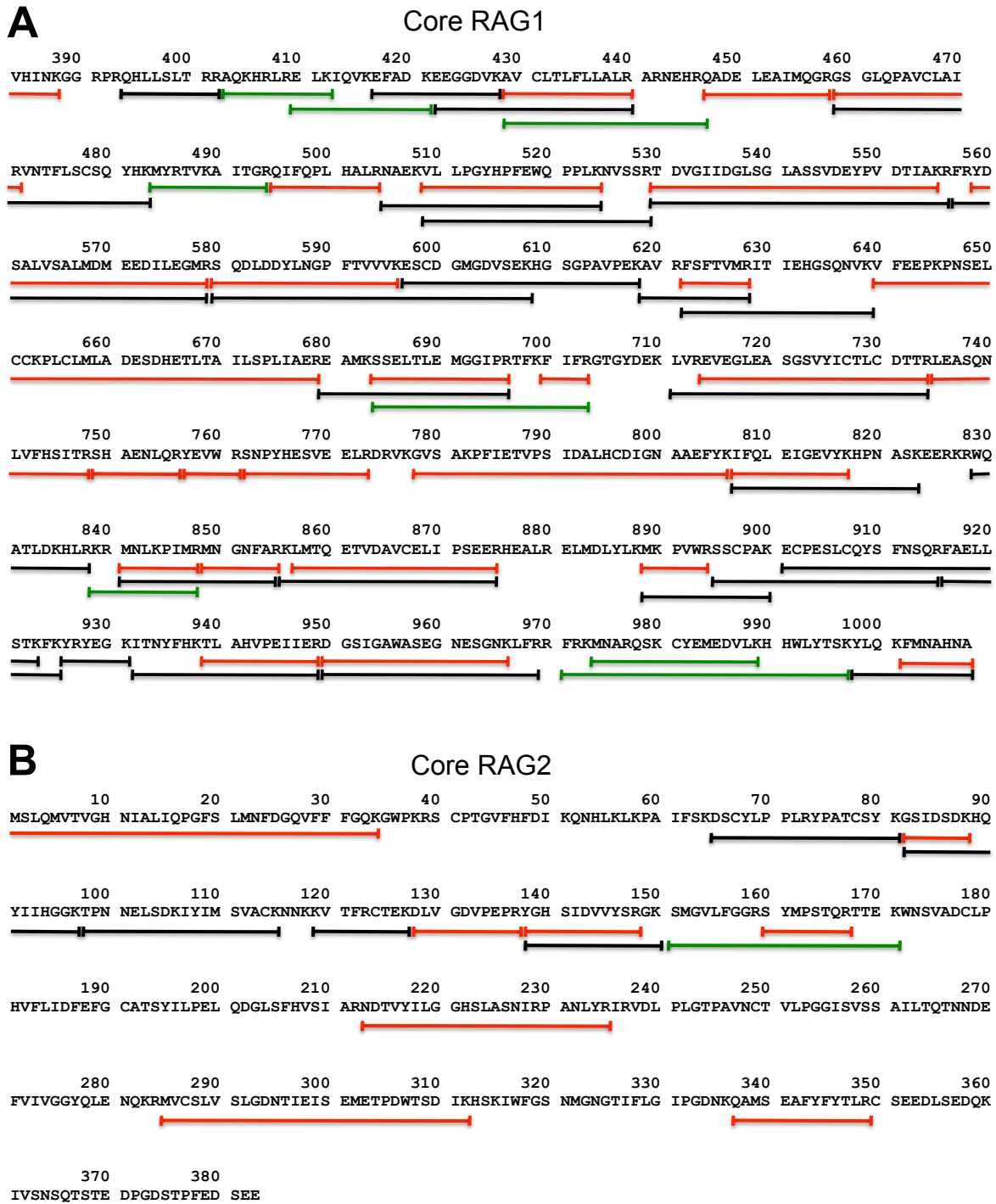


Figure S2: Amino acid sequences of **(A)** MBP-core RAG1 and **(B)** GST-core RAG2 indicating peptides identified by MALDI-TOF mass spectrometry following extensive digestion with trypsin (see Supplemental Materials and Methods). Bars beneath the sequence indicate the peptides identified by matching the m/z value of peaks from the mass spectra with the predicted monoisotopic mass values of tryptic-proteolyzed peptides in the RAG proteins. The red, black, and green bars indicate identified peptides that contained 0, 1, or 2 missed trypsin cleavage sites, respectively.

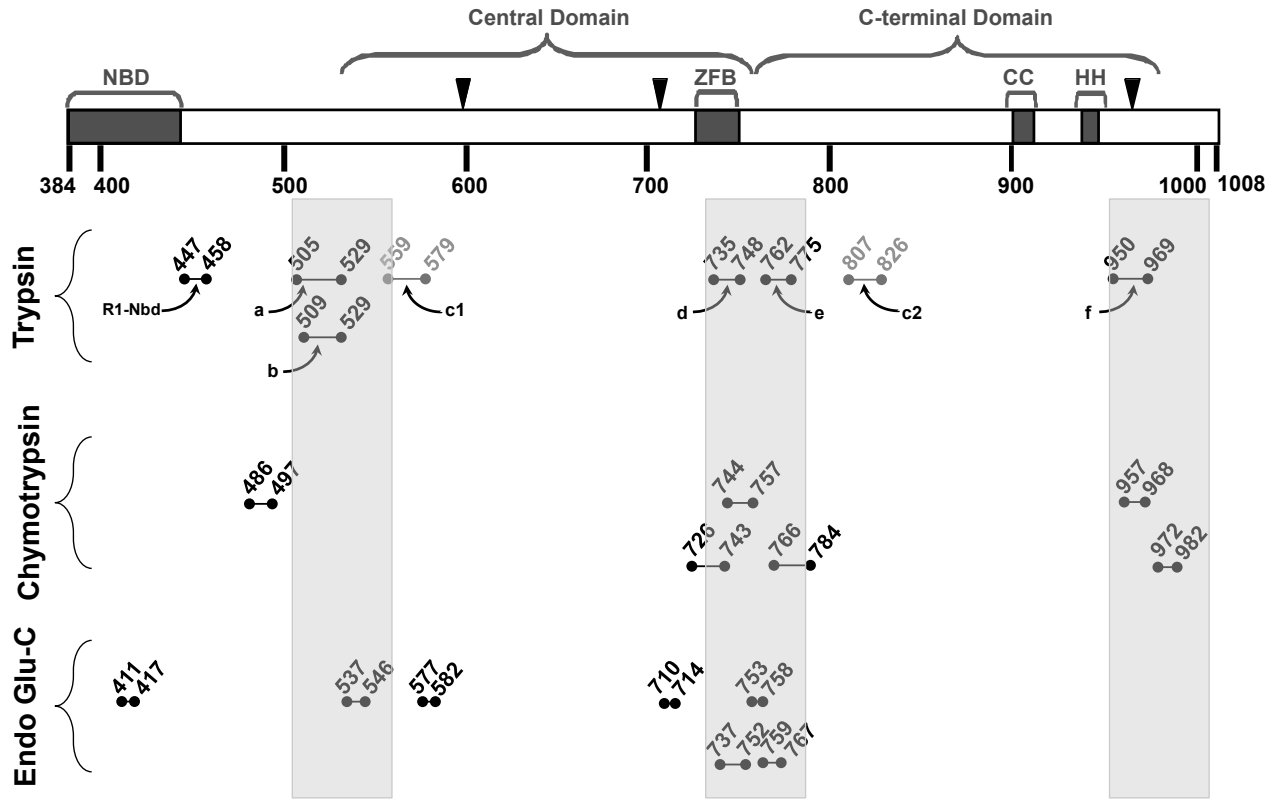


Figure S3: Assignment of surface accessible regions on core RAG1 is independent of the specific protease used in the limited proteolysis digestion. The schematic shown is as described in the legend to Figure 1C of the main text. Proteolytic peptides of core RAG1 generated by either trypsin, chymotrypsin, or endoproteinase glu-C and identified by MALDI-TOF mass spectrometry are represented by bars beneath the core RAG1 schematic.

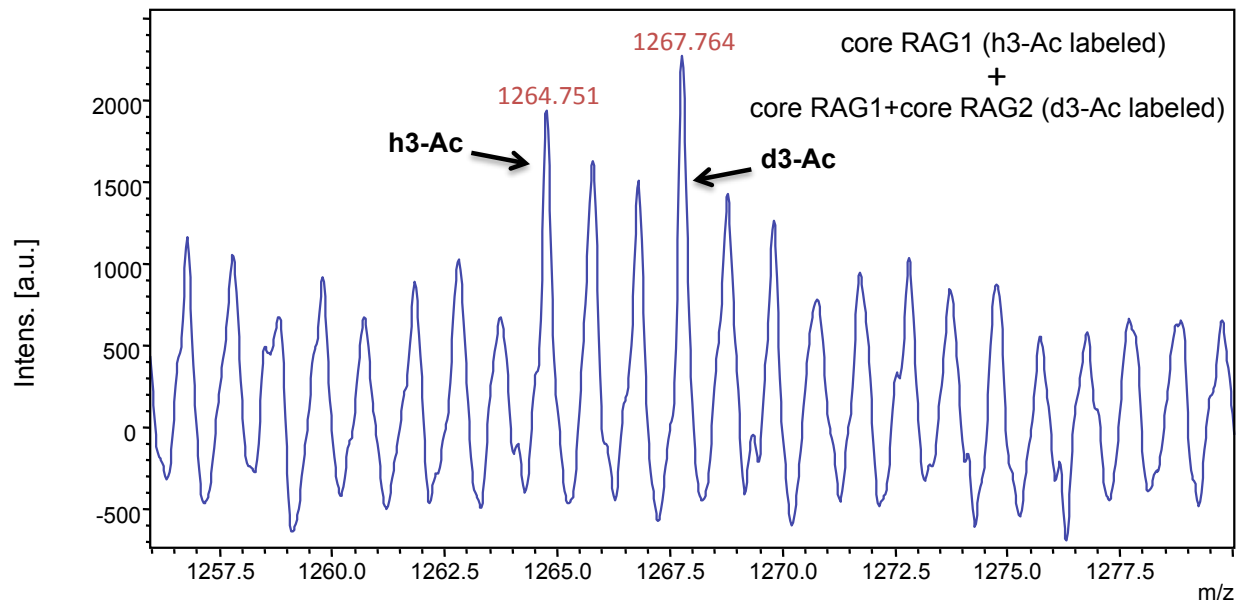


Figure S4: Isotope coding experiments indicate that the efficiency of trypsin cleavage yielding the core RAG1 peptide consisting of residues 495-504 is not affected by the presence of GST-core RAG2. Two samples consisting of 1) MBP-core RAG1 and 2) MBP-core RAG1 plus GST-core RAG2 were digested with trypsin under limiting conditions, subsequently labeled to yield h3-Ac and d3-Ac forms, respectively, and combined prior to MALDI-TOF mass spectrometry according to the method described in the main text. The peaks labeled 1264.751 and 1267.764 are the monoisotopic peaks of peptide 495-504 singly-labeled with h3-Ac (MBP-core RAG1 only sample) and d3-Ac (MBP-core RAG1 plus GST-core RAG2 sample), respectively. The ratio of the corrected d-Ac peak to the h-Ac peak was 0.95.

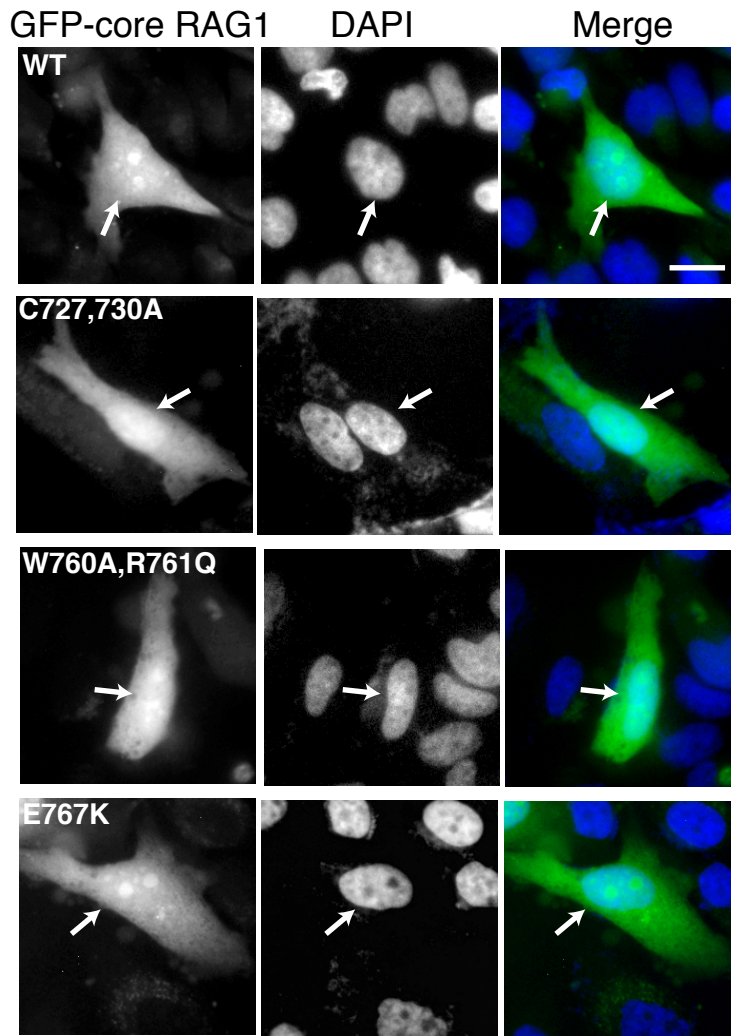


Figure S5: Mutant RAG1 proteins show similar cellular localization as wild type RAG1. Representative images of HeLa cells expressing GFP-core RAG1. The white arrows indicate the same nucleus in the GFP-core RAG1, DAPI, and merged images. White bars, 10 μ m.

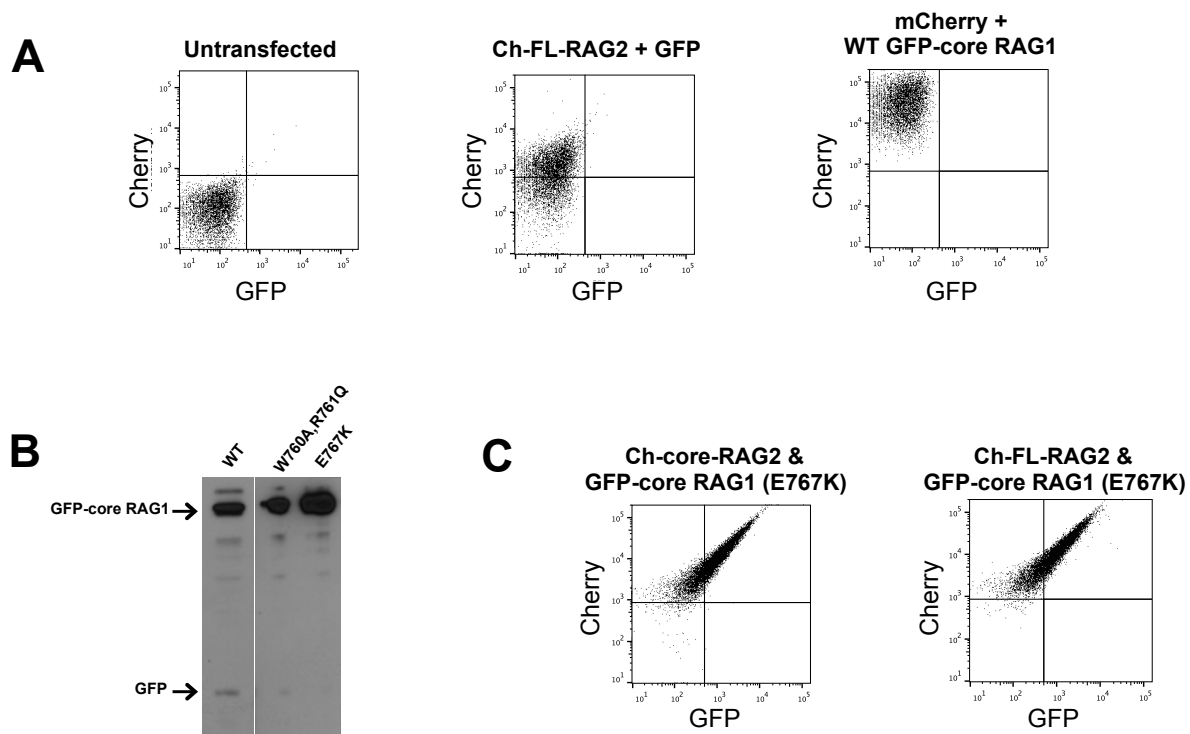


Figure S6: The fluorescence-based RFP-trap pull down assay. **(A)** Controls for fluorescence based pull down assay. Representative flow cytometry data from RFP-trap beads that were incubated with lysates from 293T cells that were mock transfected (left dot plot) or co-expressing either Ch-FL-RAG2 and GFP (middle dot plot) or mCherry and WT GFP-core RAG1 (right dot plot). **(B)** Representative Western blot using α -GFP antibody of 293T cell lysates showed negligible degradation of the fusion protein. The position of the GFP-core RAG1 and the GFP bands are indicated by arrows to the left of the blot. Intervening lanes in the blot have been removed. **(C)** Representative flow cytometry data from RFP-trap assays that analyzed 293T cells lysates coexpressing Ch-core RAG2 (left dot plot) or Ch-FL-RAG2 (right dot plot) with E767K GFP-core RAG1.

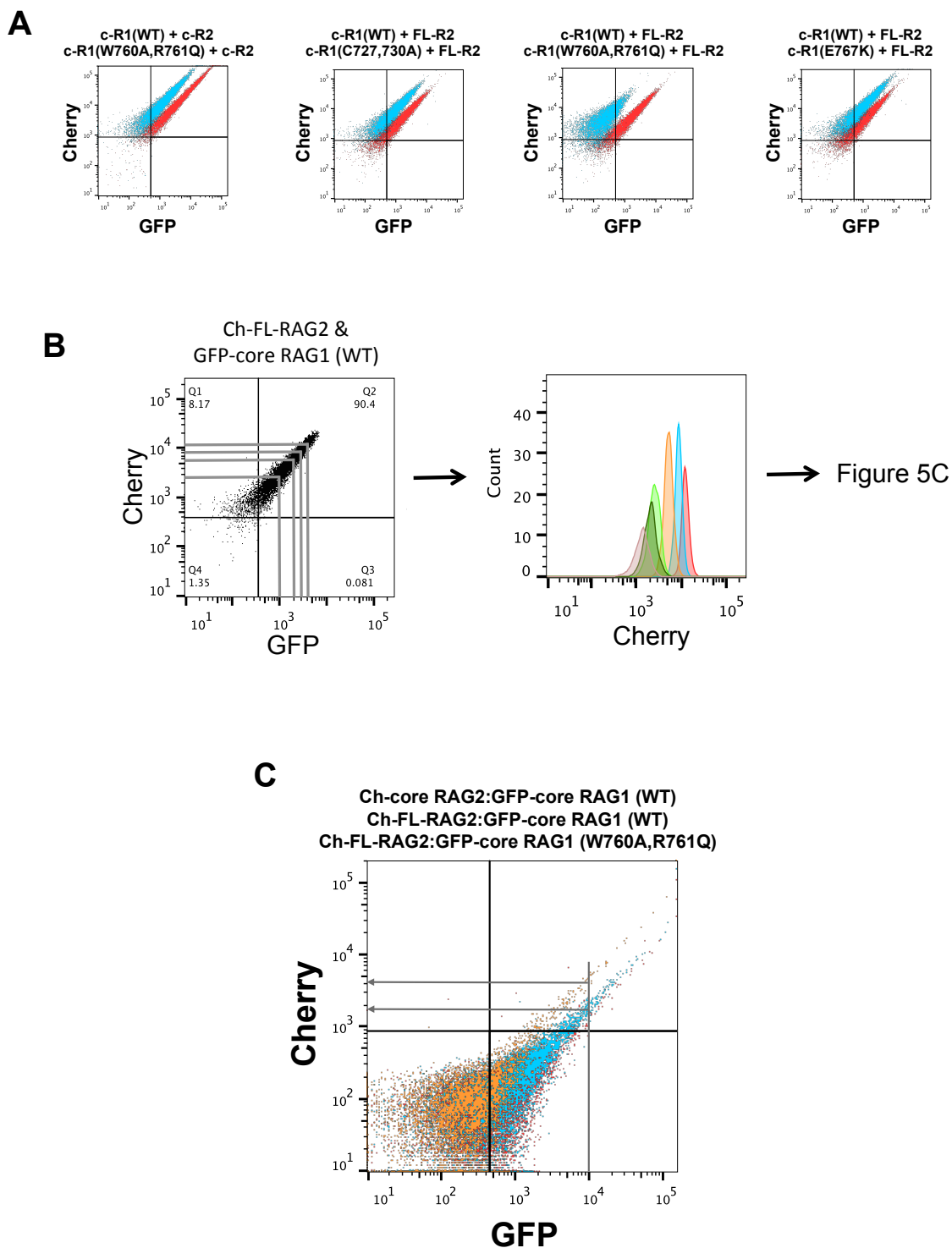


Figure S7: Determination of stoichiometric differences in RAG1 to RAG2 in V(D)J recombinase complexes containing mutant versus WT core RAG1. **(A)** Overlay of the flow cytometry data of representative experiments where RFP-trap beads were incubated with cell lysates co-expressing GFP-core RAG1 (c-R1) with either Ch-core-

RAG2 (c-R2) or Ch-FL-RAG2 (FL-R2). Experiments using WT c-R1 (red dots) are overlaid with experiments using mutant c-R1 (blue dots), as indicated. **(B)** Method for plotting normalized GFP-core RAG1:Ch-fused RAG2 complexes from RFP-trap flow cytometry results. The peak height values for the Cherry fluorescent signals at selected values for GFP fluorescence values were determined as shown in the middle plot. Each Cherry fluorescence value was normalized to that for the corresponding value from the co-expressed Ch-FL-RAG2:WT GFP-core RAG1 dataset and plotted in Figure 5C. **(C)** Overlay of representative GFP-trap flow cytometry results where GFP-trap beads were incubated with cell lysates co-expressing WT GFP-core RAG1 with either Ch-core RAG2 (blue dots) or Ch-FL-RAG2 (red dots). A third overlay is from cell lysates co-expressing Ch-FL-RAG2 with the W760A,R761Q mutant of GFP-core RAG1 (orange dots). The latter overlay shows an ~3-fold increase in stoichiometry for RAG2 to RAG1 as compared to the experiments using WT GFP-core RAG1. This difference is illustrated by the horizontal gray arrows that show an ~3-fold difference in Cherry signal (on the log scale) at the same GFP signal (vertical line) for the mutant RAG1:RAG2 complex (upper arrow) relative to the WT RAG1:RAG2 complexes (lower arrow) .